

# Economy Versus Disease Spread: Reopening Mechanisms for COVID-19

John Augustine <sup>\*</sup>   Khalid Hourani <sup>†</sup>   Anisur Rahaman Molla <sup>‡</sup>   Gopal Pandurangan <sup>§</sup>  
 Adi Pasic <sup>¶</sup>

September 21, 2020

## Abstract

We study mechanisms for reopening economic activities that explore the trade off between containing the spread of COVID-19 and maximizing economic impact. This is of current importance as many organizations (such as universities and large businesses), cities, and states are formulating reopening strategies.

Our mechanisms, referred to as *group scheduling*, are based on partitioning the population (randomly) into groups and scheduling each group on appropriate days with possible gaps (when no one is working and all are quarantined). Each group interacts with no other group and, importantly, any person who is symptomatic in a group is quarantined. Specifically, our mechanisms are characterized by three parameters  $(g, d, t)$ , where  $g$  is the number of groups,  $d$  is the number of days a group is continuously scheduled, and  $t$  is the gap between cycles.

We show that our mechanisms effectively trade off economic activity for more effective control of the COVID-19 virus. In particular, we show that the  $(2, 5, 0)$  mechanism, which partitions the population into two groups that alternatively work for five days each, flatlines the number of COVID-19 cases quite effectively, while still maintaining economic activity at 70% of pre-COVID-19 level. We also study mechanisms such as  $(2, 3, 2)$  and  $(3, 3, 0)$  that achieve a somewhat lower economic output (about 50%) at the cost of more aggressive control of the virus; these could be applicable in situations when the disease spread is more rampant in the population. We demonstrate the efficacy of our mechanisms by theoretical analysis and extensive experimental simulations on various epidemiological models.

Our mechanisms prove beneficial just by regulating human interactions. Moreover, our results show that if the disease transmission (reproductive) rate is made lower by following social distancing, mask wearing, and other public health guidelines, it can further increase the efficacy of our mechanisms.

---

<sup>\*</sup>Department of Computer Science and Engineering, Indian Institute of Technology at Madras, Chennai, Tamil Nadu, 600036, India. Email: augustine@iitm.ac.in. Research supported in part by an Extra-Mural Research Grant (file number EMR/2016/003016) funded by the Science and Engineering Research Board, Department of Science and Technology, Government of India and by the VAJRA faculty program of the Government of India.

<sup>†</sup>Department of Computer Science, University of Houston, Houston, TX 77204, USA. Email: khalid.hourani@gmail.com.

<sup>‡</sup>Indian Statistical Institute, Kolkata, 700108, India. Email: molla@isical.ac.in. Research supported by DST Inspire Faculty research grant DST/INSPIRE/04/2015/002801.

<sup>§</sup>Department of Computer Science, University of Houston, Houston, TX 77204, USA. Email: gopalpandurangan@gmail.com. Research supported, in part, by NSF grants IIS-1633720, CCF-BSF-1717075, CCF-1540512, US-Israel BSF award 2016419, and by the VAJRA faculty program of the Government of India.

<sup>¶</sup>Department of Computer Science, University of Houston, Houston, TX 77204, USA. Email: adijpasic@gmail.com.

# 1 Introduction

The COVID-19 pandemic that is sweeping the world currently has already spread to a large number of people. In many parts of the world it has already infected a significant fraction of the population. For example, in New York City, antibody testing suggests that as many as quarter of the population might be infected [9]. However, this is still nowhere near the fraction required for “herd” immunity. Many states are now starting to reopen or have already (at least partially) reopened their businesses. Large organizations such as universities and schools are also considering reopening (or already partially opening) in the Fall of 2020 and beyond. Hence, it is important to determine effective non-pharmaceutical intervention mechanisms that can safely reopen human society. Such mechanisms may significantly help in containing, controlling, and slowing the spread of COVID-19, even though it may not fully eliminate it. This will be a “new normal” wherein we learn to live with the virus, while simultaneously keeping it under control.

The goal of this paper is to study intervention mechanisms that can help in reopening society. Our main contribution is the study of a class of intervention mechanisms called *group scheduling*. The inspiration for group scheduling comes from COVID-19 characteristics whereby individuals remain asymptomatic and less infectious for around 4-5 days (the incubation period) from contraction. Subsequently, they either turn symptomatic (and can therefore be quarantined) or remain asymptomatic (and still spread the disease). Group scheduling (randomly) partitions the population (say, the students in a university or school, or the work force in a company) and schedules them (i.e., allows them to work) on different days with possible gaps (i.e., when no group is scheduled). A group is considered quarantined (at home, say) when it is not scheduled to work. Any individual who is symptomatic is quarantined as soon as he/she exhibits symptoms.

The key intuition that inspires group scheduling is that individuals can be grouped — hence reducing the number of contacts (on average) than without grouping — and scheduled to work predominantly with other less infectious individuals. Effective group schedules work in such a way that most infected individuals turn symptomatic (though a significant percentage, about 40%, may remain asymptomatic [4]) and contagious during their break – thereby facilitating quarantining before spreading the infection. On the flip side, instead of a full lockdown, our scheduling allows for significant and sustained economic activity. In fact, we showcase specific group schedules that operate at 70% of the economic activity compared to a typical five-day work week that can simultaneously dampen the spread of COVID-19 quite effectively.

The main contributions of this paper can be summarized as follows:

1. Positing and studying group scheduling mechanisms that give trade offs between economic activity and controlling disease spread (these notions are explained in Section 2).
2. Extensive analysis of various mechanisms both theoretically and by simulations. Our theoretical analysis shows why group scheduling mechanisms help in controlling COVID-19. Our simulations validate the theory and give insights into the performance of specific mechanisms.
3. Our results indicate three specific categories of mechanisms — corresponding to high, medium, and low economic activity — and their performance in controlling COVID-19. The lower the economic activity of the mechanism, the higher the control of disease. (For specific mechanisms we refer to Table 3.)
4. A main takeaway from our results is that group scheduling mechanisms help in significantly controlling the spread of COVID-19 — reducing the peak number of cases per day as well as the total number of infections. Depending on the rate of infection in a population, different mechanisms are applicable that control the disease spread while maintaining an appropriate level of economic activity.

## 2 Baseline and Proposed Mechanisms

We begin with some simple mechanisms that serve as baselines. The *basic mechanism* is one in which there is no intervention or control mechanism of any sort. The disease spreads in the population according to an underlying disease propagation model. (We consider various epidemic models as described in Section 3.) Another baseline mechanism is *symptomatic quarantining*, a widely practised mechanism wherein individuals are quarantined if they exhibit any symptom of the disease. As mentioned in Section 3, we assume that only a certain proportion of the infected individuals are symptomatic. According to current CDC estimates [4], about 60% of infected individuals are symptomatic and the rest are asymptomatic. We also consider other percentages to validate the robustness of our results.

We assume a 5 day mean incubation period (in our experiments, we consider a distribution based incubation period model for COVID-19 with mean incubation period of 5 days [14]). Individuals who exhibit symptoms are removed (quarantined) from the group. In this model, an individual will be asymptomatic with probability 0.4 (independently of others) and thus will not be removed until recovery time (assumed to be 14 days after infection); such an individual will remain contagious until they are recovered.

**Proposed Group Scheduling Mechanisms** We study a family of *group scheduling* mechanisms and highlight specific mechanisms within the family – one, in particular, that epitomizes the optimal trade off between damping COVID-19 spread and increased economic activity. Group scheduling partitions the population into different (randomly chosen) groups and schedules each group on different days with possible gaps between the schedules. A gap is when no group is scheduled. More precisely, a group scheduling mechanism is characterized by three parameters  $g, d$ , and  $t$ , where  $g$  is the number of groups,  $d$  is number of days a group is continuously scheduled, and  $t$  is the gap between the schedules. We call this a  $(g, d, t)$  *schedule*. The normal five day work week schedule is  $(1, 5, 2)$ , where the entire workforce is just one group scheduled continuously for five days with two days off. A quintessential group schedule example that we highlight is the  $(2, 5, 0)$  schedule ( $(2, 4, 0)$  also has quite similar performance with the same economic output — see below). It partitions individuals into two groups scheduled alternatively for five days each without any break between cycles. Thus, individuals cycle between five days of work and five days (quarantined) at home.

We evaluate our mechanisms in two main aspects:

1. How disease spreads under the mechanism and comparing it with simple baseline mechanisms. In particular, we posit the so-called *flattening ratio* which is the ratio of the peak number of cases (during the course of the epidemic simulation) under our mechanism compared to the peak number of cases under a baseline mechanism, e.g., the normal 5-day work week.
2. The economic output of the mechanism characterized by what we call as the *work output* or *economic ratio* defined as the *ratio* of the average number of working hours of an individual under our mechanism to the average number of working hours under the standard five-day working week (i.e., the  $(1, 5, 2)$  schedule).<sup>1</sup> For a mechanism with parameters  $(g, d, t)$ , the economic ratio is computed by the formula (see Appendix for a derivation):

$$\frac{7}{5} \left( \frac{d}{gd + t} \right)$$

The economic ratio for a normal work week, i.e., the  $(1, 5, 2)$  schedule, is 100%, whereas for the  $(2, 4, 0)$  (and  $(2, 5, 0)$ ) schedule it is 70%.

There are two advantages in group scheduling: (1) the average number of contacts per group is reduced by a factor of  $1/g$  (compared to a single group) which means that less individuals are infected by an infected

---

<sup>1</sup>We assume that an individual works for a fixed number of hours (say, 8) on each day they are working.

person on average per day; (2) Since infected symptomatic individuals in a group are quarantined when they are not scheduled, this means that the number of days a person is infectious is reduced. Thus even when the number of groups is relatively small (say 2, 3, or 4) and even for small  $d$  and  $t$  values, the spread of disease is significantly reduced, while still keeping the economic ratio reasonable.

We demonstrate the efficacy of our mechanisms both theoretically (cf. Section 4) and experimentally (cf. Section 5). For our theoretical analysis, we consider a simple branching process model and analyze how the disease spreads as a function of the mechanism parameters ( $g$ ,  $d$ , and  $t$ ) and the COVID-19 disease parameters. Our analysis is fruitful in determining what mechanisms are likely to work well and also gives insight into our simulation results on various epidemiological models, which we discuss next.

### 3 Models, Assumptions, and Parameters

Infectious diseases such as COVID-19 spread by contacts between people. While various factors influence the spread of diseases, including COVID-19, we focus on a key ingredient that contributes to the spread of disease: the number of contacts between people and the distribution of the number of contacts (some people may have significantly more contacts than average). We simulate our mechanisms under two different types of standard epidemiological models: network-based and random-mixing based [13]. Network-based models use an underlying *fixed graph structure* that determines the disease propagation, while random mixing models such as the traditional differential equations-based SIR (or SEIR) allow contacts between random individuals in the population (though the average number of contacts might be the same in both models). *We show that our mechanisms gives qualitatively similar benefits regardless of the specific models used in our simulations as well as the specific choice of parameters of the respective models.* These are discussed in detail in Section 5.

**Network-based Contact Models** We use a simple graph-based model that is based on contact distribution from real-world data [15]. The work of [15] was a fairly large-scale (involving 7290 individuals and 92,904 contacts), population-based survey of “epidemiologically relevant” social contact patterns.

We define a *contact graph* where nodes consist of individuals and edges (assumed to be undirected) denote contacts between them. To model spatial distribution, we assume that nodes are distributed randomly in a unit area (square). This is a variant of the *random geometric graph* model that has been extensively studied [16]. In this random geometric graph model that we call the  $G(n, k)$  model, we have  $n$  nodes uniformly distributed in a unit area and each node has an edge with its  $k$  closest neighbors. Note that this model has two key features: (1) spatial locality — edges are between nodes that are in proximity (2) the small-world property — neighbors of a node are themselves likely to be connected.

One might point out that having a uniform distribution of nodes (people) is not really reflective of the real world. While true, we posit that this is of lesser importance, especially when restricted to modelling densely populated areas such as Manhattan or Dharavi (Mumbai), or a university or a industrial workplace. However, more important is the modelling of the *contacts between people*.<sup>2</sup> Hence, instead of adding an edge between a node and its  $k$  closest contacts, where  $k$  is fixed for all nodes, we use the well-studied real-world data for contact distribution due to [15] to sample the number of contacts  $k(v)$  for each node  $v$ . For a node  $v$ ,  $k(v)$  is its degree in the contact graph and its neighbors constitute the set of individuals that  $v$  can infect directly. The work of [15] studied the number of contacts for over 7000 people across eight countries in Europe. This data gives a contact distribution for the number of contacts of each node *per day*. *The mean number of contacts for a person per day, that we denoted as  $C$ , according to this distribution is 13.4.* We

---

<sup>2</sup>In any case, as mentioned earlier, it is important to point out that the efficacy of the mechanisms are qualitatively similar regardless of the models, in particular whether it is contact-graph based or random mixing-based. Even in contact-based model, we consider models where geometry is less important, as discussed later.

note that this contact distribution is for “normal” human behavior (i.e., no social distancing, quarantining, etc.).

We also consider an alternative contact graph model that is based solely on the contact distribution and *ignores the underlying geometry*. We call this  $G'(n, D)$  model. It is a variant of a well-studied random graph model called the *Chung-Lu model* that is based on degree distribution [5]. Formally, the  $G'(n, D)$  model (which is also undirected) is defined as follows. For each node  $v$ , we sample the (expected) degree of  $v$ ,  $d(v)$ , from the contact distribution  $D$ . We then construct a *random graph* as follows. For each pair of nodes  $u$  and  $v$ , an edge is added between  $u$  and  $v$  independently with probability  $d(u)d(v)/\sum_u d(u)$ . Note that, under this model, the expected degree of  $v$  is equal to  $d(v)$ . We note that one important difference between the random geometric graph model and the random graph model, is that the diameter of the Chung-Lu model is substantially smaller (about logarithmic in the size of the graph) than the random geometric graph. This means that the disease can potentially spread faster among the population, since there are shorter paths between nodes.

Finally, we also consider a parameterized hybrid model that interpolates between the random geometric model and the Chung-Lu random graph model, depending on a parameter  $p$ . In this model, each node has a degree (say  $d$ ) randomly chosen from a distribution. The  $d$  neighbors are then chosen as follows – with probability  $p$ , the *next closest neighbor* (in the geometric sense) is chosen as a neighbor of the node. With probability  $1 - p$ , the neighbor is chosen randomly from *all nodes* in a weighted distribution with weights proportional to the degree of each node (in the Chung-Lu sense).

**COVID-19 Disease Model** We now discuss how we model the spread of disease on the underlying contact graph. We employ a parameter called the *transmission probability*,  $T_p$ , the probability that an infected node infects each of its uninfected contacts (neighbors in the contact graph) on *any given day*. Note that the  $T_p$  value is related to the commonly used *reproductive rate* (or *effective reproductive rate*)  $R(t)$  which measures on (average) the number of individuals an infected individual infects over the course of his/her infection (at any particular time  $t$  during the epidemic). For the contact-graph model, one can approximately relate  $T_p$  and  $R(t)$  as follows (See Appendix for a derivation):

$$R(t) = (1 - (1 - T_p)^D) \times C$$

where  $C$ , as defined earlier, is the (average) number of contacts per person (we assume this value to be 13.4 throughout this paper based on [15] data) and  $D$  is the (average) number of days a person remains infectious (we assume in this paper that this number is 11 days for COVID-19 [8]). Note that in the contact graph model, since the underlying graph structure is fixed,  $R(t)$  generally cannot exceed  $C$ . For a random mixing model, the relationship between  $T_p$  and  $R(t)$  is somewhat different (cf. Section 3). For example, currently for Houston, the reproductive rate is around 1 and this means that  $T_p$  value under the above model is (approximately) 0.007 (assuming  $C = 13.4$  and  $D = 11$ ). Generally, the reproductive rate of COVID-19 is estimated to be less than 3 [8] and this corresponds to  $T_p = 0.022$  (approximately) in the above contact graph model.

While the traditional approach in epidemiological modelling is to predict disease spread by estimating  $T_p$  or  $R(t)$  values and fitting these estimates in a model, we do not estimate these values. Rather, we study our mechanisms under various possible values for  $T_p$ : we compare the effectiveness of our mechanisms under different possible values with the baseline mechanisms discussed earlier. A high  $T_p$  value means that the disease is spreading rampantly, while a low value means that the disease is spreading relatively slowly. We show that regardless of the value of  $T_p$ , our specific group scheduling mechanisms significantly reduce the infection spread compared to the baseline mechanisms. However, the efficacy increases even more as the  $T_p$  values decrease (cf. Section 5).

For modeling the disease progress, we adopt an *SEIR model*, where individuals can be in four categories. Initially all individuals are considered *Susceptible* to the disease. When a susceptible individual becomes

infected, they first enter an *Exposed* state, wherein the individual is not contagious. After a period of time, the individual then enters the *Infected* state. During the infected state, an individual can transmit the disease with probability  $T_p$  per contact per day. Then, after a certain period (called the *recovery time*), the individual becomes *Removed* (i.e., either recovered or deceased).<sup>3</sup> A removed individual cannot spread the infection to its neighbors.

We start with a set of randomly chosen individuals — called the *index set* — infected at the beginning of the simulation. We assume that the size of the index set is proportional to the *current* size of infected individuals in the population (e.g. in Harris County, Texas, it is about 3% in August 2020 [10]).

The *Incubation period* is the time between becoming infected and the development of symptoms. On average, it is estimated that, for COVID-19, it is 5.1 days, but can vary from 2-14 days [8, 14]. For our simulations, we use a distribution-based model for incubation period for COVID-19 [14]: we assume that the incubation period is given by a lognormal distribution with mean (approximately) 5 (days).

We assume that an infected person becomes contagious 2 days before the incubation period [8]. After a person becomes contagious, they can infect each of their contacts with probability  $T_p$  per day. We consider various values of  $T_p$  ranging from very high (say, 0.5) to relatively low (say, 0.01) — as mentioned earlier, one can directly relate  $T_p$  to the reproductive rate. After 14 days recovery time, an individual is *Removed* (i.e., either recovered or deceased). A removed individual is assumed to not be contagious.

It is known that *asymptomatic* carriers of COVID-19 play a significant role in the spread of the disease. It is estimated that as many as 40% of infected individuals are *asymptomatic*, i.e., they do not show any symptoms, but continue to infect their contacts until they become *Removed*. We assume a similar estimate in our analysis, i.e., we assume each infected individual is asymptomatic with probability 0.4 (independently of others). We assume that asymptomatic carriers are as infectious as symptomatic carriers and become infectious in a similar time frame (i.e., two days before the incubation period, though they do not show symptoms).

Parameter	Definition	Value Used in our Analysis
$T_p$	probability that a contagious person infects a single neighbor in a day	{0.01, 0.1}
asypm	probability that an infected person is asymptomatic	0.4
incubation period	number of days until symptoms develop from infection	5
$C$	number of contacts per person	13.4
$D$	number of days an infected person remains infectious	11

Table 1: COVID-19 parameters used in our analysis.

**Random mixing model** To study the robustness of our mechanisms across different models, besides the contact graph models and its variants described earlier, we also consider a classical SEIR random mixing model. The SEIR model tracks stages of a disease; susceptible, exposed, infected, and recovered, as the number of individuals in each stage. The evolution of each compartment is regulated by standard differential equations (see e.g., [13]). We use a variation of the classical SEIR model with a lognormal distribution

<sup>3</sup>We ignore “deceased” in our simulations as these are quite small.

for the incubation period. The random mixing model allow each individual to have contact with random individuals which enables the possibility of larger values for the reproductive rate  $R(t)$  since any susceptible individual can become exposed. (By contrast, the contact graph model limits the susceptible population to the subset of nodes adjacent to infectious carriers.) One can relate  $R(t)$  and  $T_p$  as:  $R(t) = T_p \times C \times D$ .

## 4 Theoretical Analysis of Mechanisms

We present a theoretical analysis assuming a simplified model which is easier to analyze than the contact graph models defined earlier. A main goal of our analysis is to study the efficacy of mechanisms with respect to disease spread. In particular, given a value of transmission rate  $T_p$ , we would like to discover mechanisms (with good economic ratio) that can effectively control the spread of disease. The evolution of the disease depends on the transmission rate  $T_p$  (higher the  $T_p$ , more is the rate of spread), the number of contacts per individual, the number of days a person is infectious, and the asymptomatic rate. It is important to note that our mechanisms employ symptomatic quarantine and hence symptomatic individuals contribute less to the spread (since they are infectious for a short while before symptoms show up and they get quarantined). However, asymptomatic carriers who constitute about 40% of infected individuals play a major role in spreading the disease. We analyze how the disease spreads under a given  $(g, d, t)$  mechanism.

Our analysis uses the well-known Galton-Watson branching process (e.g., see Section 8.1 [11]) to study the disease evolution. In a branching process, each (infected) individual independently infects an  $X$  number of individuals, where  $X$  is a random variable (captures the reproductive rate) with a fixed distribution (with finite mean and variance). The new set of infected individuals belong to the next generation.

In a branching process analysis, we start with an infected individual and study how the number of infected individuals grow in each generation. Table 1 lists the key parameters (and their typical values) used in our analysis.

Consider an infected individual, say node  $v$ . By our modeling assumptions,  $v$  will be symptomatic with probability 0.6 and asymptomatic with probability 0.4. Let  $\mu_s$  (resp.  $\mu_a$ ) be the expected number of people that are infected by a symptomatic (resp. asymptomatic) infected individual. Essentially,  $\mu_s$  and  $\mu_a$  are the effective reproductive rates  $R(t)$  for the symptomatic and asymptomatic patient respectively. Let  $X_i$  be the random variable counting the number of infected people at the  $i^{th}$  generation and  $E(X_i)$  be the expected value of  $X_i$ . Assuming  $X_0 = 1$ ,  $E(X_1) = (0.6\mu_s + 0.4\mu_a)$ , and in general,  $E(X_i) = (0.6\mu_s + 0.4\mu_a)^i$ , which follows from the branching process (a formal argument can be found in [11]). See Figure 1.

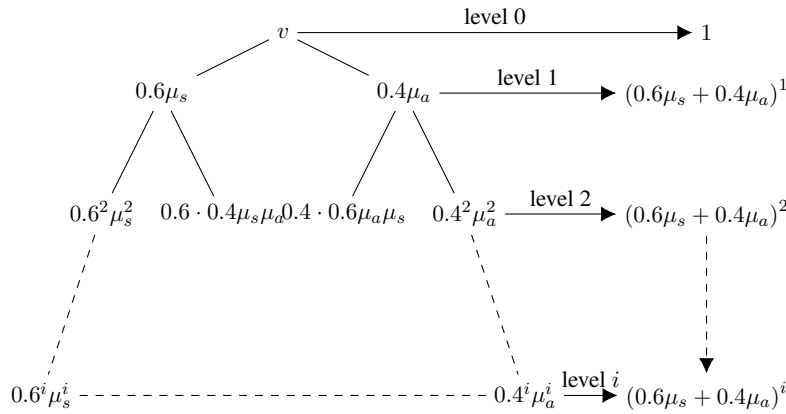


Figure 1: Illustrating the branching process analysis. The right hand side displays the total expected number of infected people at each level.

Thus, the expected total number of infected individuals is  $\sum_{i=1}^{\infty} (0.6\mu_s + 0.4\mu_a)^i$  which is a geometric series sum. Therefore, if  $(0.6\mu_s + 0.4\mu_a) < 1$ , i.e., each individual infects less than one person on average, then  $E(X_i) \rightarrow 0$  as  $i \rightarrow \infty$ . In this case, the disease dies out eventually. But if  $(0.6\mu_s + 0.4\mu_a) > 1$  (i.e., each individual infects more than one person on average), then  $E(X_i)$  grows exponentially fast. In this case, the disease-spread explodes and infects everybody eventually. Thus we get the following theorem.

**Theorem 1.** *If  $(0.6\mu_s + 0.4\mu_a) < 1$  then the branching process dies out eventually, i.e., the disease stops spreading further.*

Below we calculate the value of effective reproductive rate  $(0.6\mu_s + 0.4\mu_a)$  for the general mechanism  $(g, d, t)$ . Then we analyze different specific mechanisms to check whether the disease dies out or not under the mechanism.

In the random mixing model, the reproductive rate is  $R(t) = T_p \times D \times C$ , where (recall that)  $T_p$  is the transmission probability,  $D$  is number of days a person remains infectious and  $C$  is the number of contacts per person. By considering a schedule  $(g, d, t)$ , the above formula becomes:

$$R(t) = T_p \times D^g \times C^g, \quad (1)$$

where  $C^g = C/g$  is the number of contacts in a random grouping of  $g$  groups and  $D^g$  is the number of days a person is infectious as determined by the schedule (note that if a group is not scheduled, then any person in that group is not considered infectious, even though he/she may be infected). The following lemmas compute the symptomatic and asymptomatic reproductive rates for a  $(g, d, t)$  mechanism. The proofs are derived from Equ 1 with appropriate calculation of  $D^g$  and  $C^g$ , but are placed in the Appendix.

**Lemma 1.** *Let  $d' = \max\{0, \min\{d - 2, 5\}\}$  and  $d'_i = \max\{0, \min\{5 - (gd + t)i, d\}\}$ . Then the Symptomatic reproductive rate is given by:*

$$\mu_s = \frac{(13.4)T_p}{g} \cdot \left( d' + \sum_i d'_i \right)$$

**Lemma 2.** *Let  $d'' = \max\{0, \min\{d - 2, 11\}\}$  and  $d''_i = \max\{0, \min\{11 - (gd + t)i, d\}\}$ . Then our Asymptomatic reproductive rate is given by:*

$$\mu_a = \frac{(13.4)T_p}{g} \cdot \left( d'' + \sum_i d''_i \right)$$

Thus, one can calculate  $(0.6\mu_s + 0.4\mu_a)$  from the above formulas. Table 2 computes this value for different mechanisms for two different  $T_p$  values — 0.1 (high) and 0.01 (low). If the value of  $0.6\mu_s + 0.4\mu_a < 1$  for a mechanism and a  $T_p$  value, then the disease dies out; moreover, closer this value is to 0, the faster the disease dies out (and ends up infecting a smaller fraction of the population). These predictions are validated by simulation results (Section 5).

## 5 Simulation Results

To study the efficacy of our mechanisms, we also conduct extensive simulations across various models and parameters. For example, given a particular mechanism, say  $(2, 4, 0)$ , we simulate the disease spread under this mechanism under various models (the contact graph model and its variants, and the random mixing model). Under each model, we vary the following parameters to study their effects. We vary transmission probability  $T_p$  (which captures the rate of infection spread in the population), the number of index patients (which captures the percentage of individuals currently infected among the population), and the percentage



$T_p$	Schedule			
	(1, 5, 2)	(2, 5, 0)	(3, 3, 0)	(4, 4, 0)
0.01	0.616	0.228	0.080	0.067
0.10	6.164	2.278	0.804	0.670

Table 2: Values of  $0.6\mu_s + 0.4\mu_a$  for different values of  $T_p$  and schedules  $(g, d, t)$ . A green box indicates that the process eventually dies out, whereas a red box indicates continued growth.

of asymptomatic carriers (we assume this to be 40% according to current estimates [4], but we also try other values). We then compare the disease spread, under the *same set of respective parameters*, to three baseline mechanisms — the basic model (where the diseases spreads without any intervention), symptomatic quarantine or the (1, 1, 0) schedule (where infected individuals are quarantined after exhibiting symptoms), and the (1, 5, 2) schedule, which is the normal 5-day work week with symptomatic quarantine (note that in the latter two mechanisms there is only one group). The key metric of comparison is the flattening ratio — the ratio of the peak number of cases of the mechanism under consideration (say (2, 4, 0)) to that of the baseline mechanisms. (We also compare the total number of infections as well.)

We analyze a number of group scheduling mechanisms that showcase the trade off between economic ratio and the disease spread. We categorize them into three broad groups as: (i) high-ER mechanisms ( $\sim 70\%$  economic ratio), (ii) mid-ER mechanisms (40 – 50%), and (iii) low-ER mechanisms (about 30%).

Our results are summarized in Figures 2 and 3 and Table 3. These particular results assume a population of 50,000 (typical population in a large university) and the number of index patients is 3% of the population (i.e., 3% of the population is initially infected as is currently estimated in Harris County, TX [10]). The simulation model is the random geometric model with the contact distribution as described in Section 3. We adopt the COVID-19 disease parameters as described in Section 3. Our results are *qualitatively similar* across the various models including the random mixing model and other variants of the contact graph model. We have simulated higher populations (up to 100,000 in the contact graph model, and up to million in the random mixing model) and have varied the number of index patients. More importantly, we have analyzed a wide variety of  $T_p$  values — here we consider two canonical  $T_p$  values — 0.1 and 0.01 — these capture high and low reproductive rates respectively (cf. Section 3).

Our results can be summarized as follows (see Figures 2 and 3). The canonical example for the high-ER category is the (2, 5, 0) schedule, which achieves a (1, 5, 2) flattening ratio as low as 12% (i.e., the ratio of the peak number of cases is 12% compared to that of the standard work week schedule) even when  $T_p = 0.1$ . When  $T_p$  is lower, say around 0.01 the flattening ratio becomes much lower. (In general, lower the  $T_p$ , the better the flattening, in general, for any given mechanism.) In fact, several mechanisms of the form (2,  $d$ , 0) yield the same economic ratio and essentially the same flattening ratio for  $d \geq 4$ . In the mid-ER category, we get even better flattening ratios. The canonical example for this case is (3, 3, 0) yielding an economic ratio of 46%, but with the flattening ratio down to 4% even under  $T_p = 0.1$ . For mechanisms in low-ER category, such as (4, 4, 0) with still a reasonable economic ratio of 35%, the flattening is down to about 1%. The mid-ER and low-ER mechanisms are attractive when  $T_p$  values are high, as they not only lead to a low flattening ration, but also low number of peak cases (in absolute numbers) with respect to the total population. Moreover, the total number of infections is a small fraction of the total population.

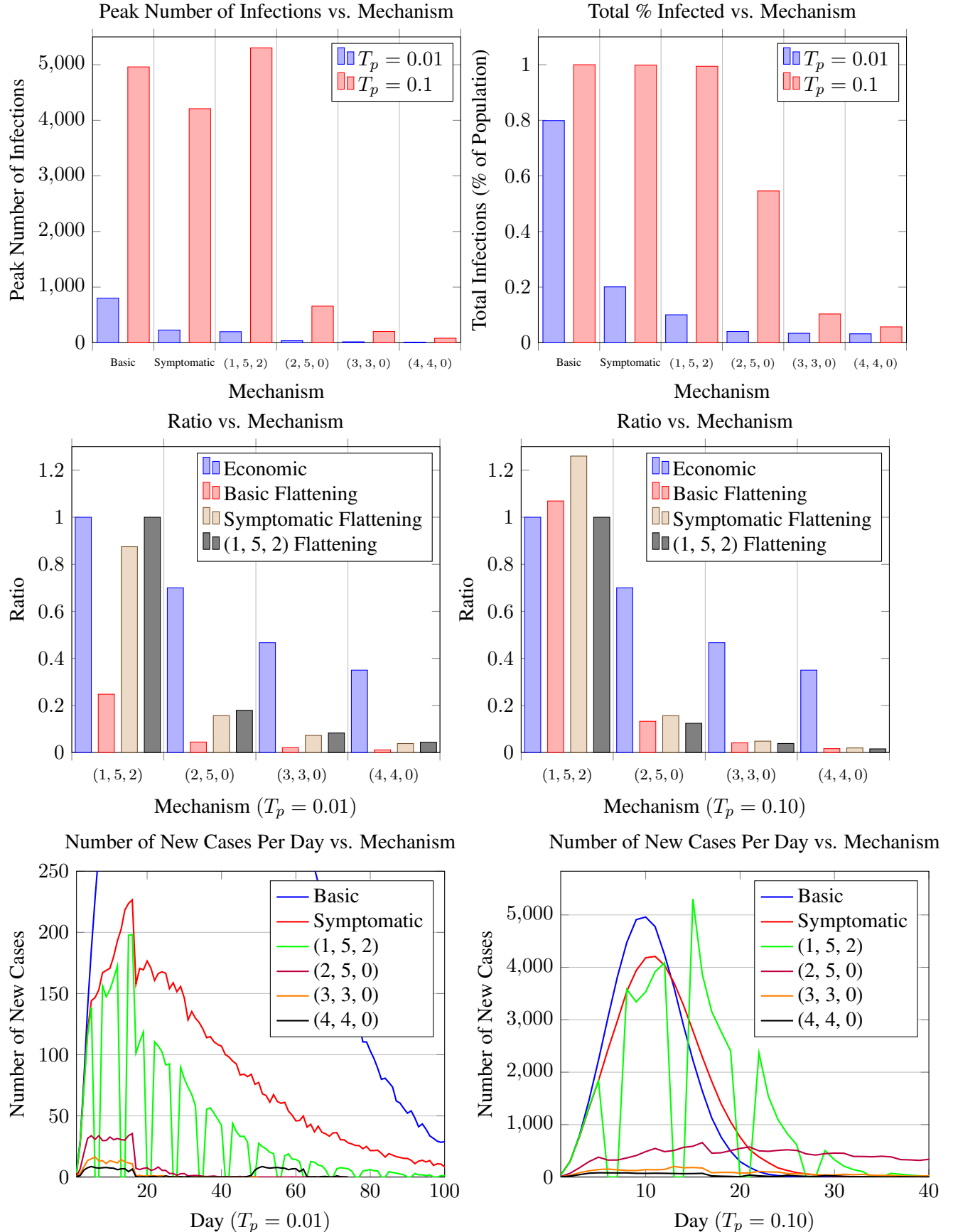


Figure 2: Plots displaying the performance of different mechanisms for Contact Graph Model.

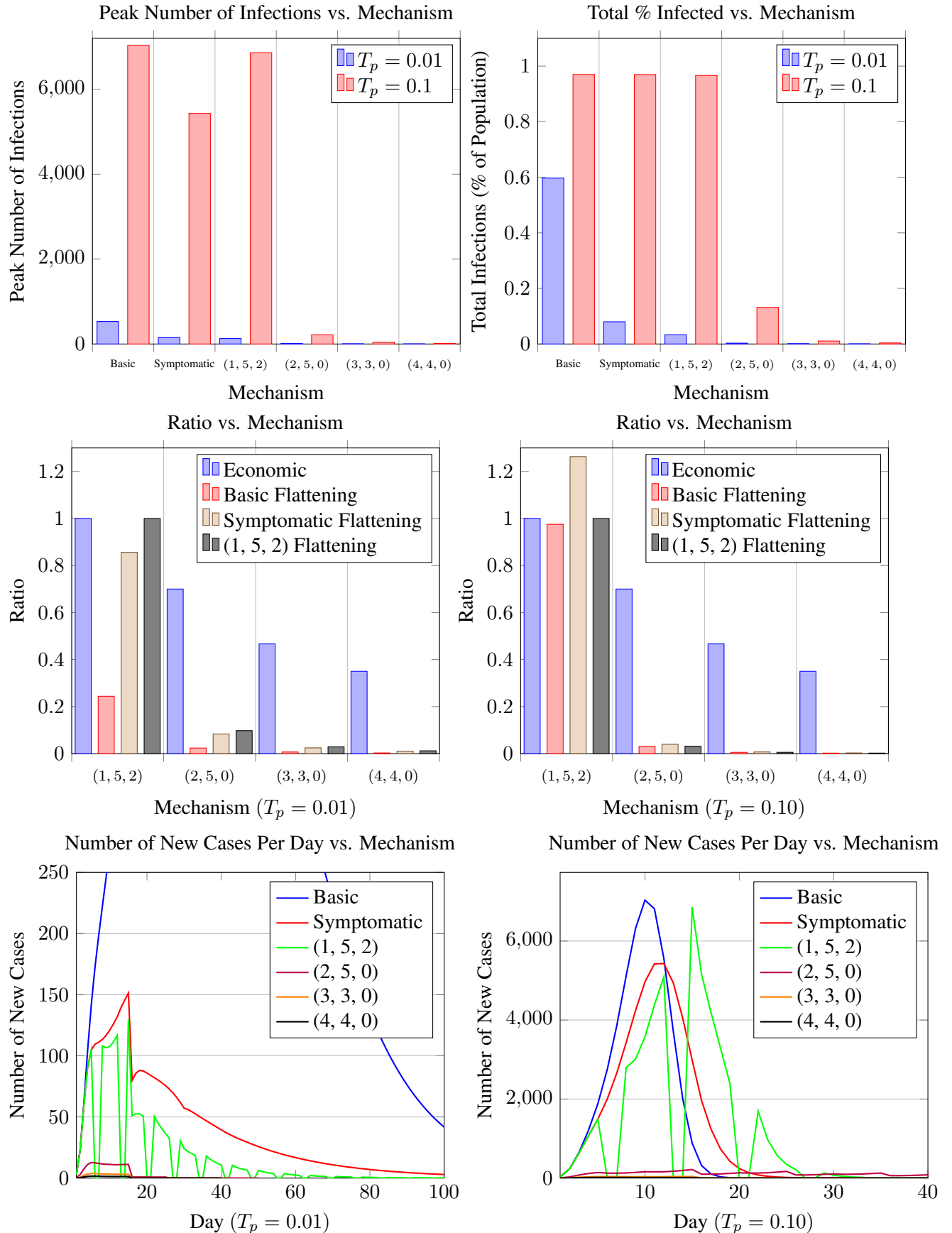


Figure 3: Plots displaying the performance of different mechanisms for SEIR Model.

ER Category	Schedule	ER	$T_p = 0.01$			$T_p = 0.1$		
			Basic	Sympt.	(1, 5, 2)	Basic	Sympt.	(1, 5, 2)
Full	(1, 5, 2)	100%	23%	80%		107%	127%	
	(1, 1, 0)	140%	29%		124%	84%		79%
High	(2, 4, 0)	70%	4%	14%	18%	14%	17%	13%
	(2, 5, 0)	70%	4%	14%	18%	12%	15%	12%
Mid	(2, 3, 2)	53%	4%	15%	18%	11%	14%	11%
	(2, 3, 3)	46.7%	4%	14%	18%	11%	13%	10%
	(3, 3, 0)	46.7%	2%	7%	8%	4%	5%	4%
Low	(4, 4, 0)	35%	1%	3%	4%	2%	2%	1%

Table 3: Economic and flattening ratios for various schedules against the Basic, Symptomatic Quarantine, and (1, 5, 2) mechanisms for  $T_p$  values of 0.01 and 0.1. A higher economic ratio indicates more economic output, whereas a lower flattening ratio indicates a lower peak number of new cases per day.

## 6 Related Work

Our work closely resembles several recent papers on cyclical strategies [12, 2, 7]. A typical cyclical strategy parameterized by  $1 \leq k < 14$  views 14 days as one work cycle and stipulates that the population works for  $k$  days followed by  $14 - k$  days of lockdown. Our work is complementary to their works. The key difference is that our group scheduling mechanisms benefit significantly from the reduced number of contacts owing to the partitioning of the population whereas the cyclical mechanisms typically do not. Moreover, our approach to modeling the economic impact is much simpler than the works by [2, 7] and quite likely to be more intuitive and easy for policy makers to reason about and compare alternatives.

We note that [12] briefly discusses a staggered form of cyclical strategies. Apart from being primarily focused on typical cyclical strategies, [12] do not provide any careful trade off analysis with respect to the impact on the economy. [2] provides a detailed model that studies the trade off between the effectiveness of typical cyclical strategies and the economy. However, we believe that our group scheduling mechanisms can provide significantly better trade off. There has been a flurry of recent works like [1, 3, 6] that study other mechanisms like social distancing and targeted lockdowns in the context of their related economic impact.

## 7 Concluding Remarks

Our results crucially imply the existence of mechanisms that can trade off between their effectiveness in damping the spread of COVID-19 and the work output ratio. The mechanisms we study are elementary and can be easily coupled with other policies such as social distancing and wearing face masks that can further reduce the spread of COVID-19. For convenience, we have categorized our mechanisms based on their economic ratios. The low end of this spectrum provides the best flattening ratio. So naturally, when case surge (characterized by a higher transmission probability or reproductive rate) or when easing out of complete lockdown, we may wish to opt for the low economic ratio options that have improved flattening ratio. As case numbers improve, we have a couple of strategies that we can trade between. On the one hand, low case numbers afford us the ability to contact trace more effectively and thereby stomp the spread. On the other hand, we can also move to mechanisms with improved economic ratio. As demonstrated by our

results, if the transmission probability is reduced, then the peak number of cases (as well as the total number of cases, in many mechanisms) goes down significantly. Following social distancing and mask wearing and other public health guidelines, reduces the transmission probability and thus increases the efficacy of the mechanisms, allowing deployment of high-ER mechanisms as well.

We are guided by two main principles. Firstly, our mechanisms – by partitioning the population into groups – reduce the number of contacts. Secondly, we our strategies schedule employees to with sufficient breaks so that a large number of infected persons become symptomatic (and therefore quarantined) during their breaks.

We believe that policy makers can be guided by these principles taking other local constraints into consideration. In general, a policy A that (with respect to another policy B) either decreases the number of contacts and/or improves the probability that people become symptomatic during their break will dominate over B and lead to better flattening. This means that adding common work-breaks – e.g., Sundays off – is likely to improve the flattening ratio and unlikely to worsen it. Policy makers can use the above two principles to address scenarios that we have not addressed directly. Shift workers, for example, may need to work on a more fine-grained schedule. Consider a shift schedule that requires two shifts per day. We could consider four groups with each alternating between four working days and four off days. The groups may be staggered so that – on any given day – two groups are working and two are off.

## References

- [1] Daron Acemoglu et al. *A multi-risk SIR model with optimally targeted lockdown*. Tech. rep. National Bureau of Economic Research, 2020. URL: <https://www.nber.org/papers/w27102.pdf>.
- [2] Uri Alon et al. *COVID-19: Looking for the Exit*. Tech. rep. 2020. URL: <https://www.tau.ac.il/~yashiv/LS>
- [3] Luiz Brotherhood et al. *An economic model of the Covid-19 epidemic: The importance of testing and age-specific policies*. IZA Discussion Paper No. 13265. 2020. URL: <https://www.iza.org/publications/c>
- [4] *COVID-19 Pandemic Planning Scenarios*. (accessed September 3, 2020). 2020. URL: <https://www.cdc.gov/co>
- [5] Fan Chung and Linyuan Lu. *Complex Graphs and Networks (Cbms Regional Conference Series in Mathematics)*. USA: American Mathematical Society, 2006. ISBN: 0821836579.
- [6] Martin S Eichenbaum, Sergio Rebelo, and Mathias Trabandt. *The macroeconomics of epidemics*. Tech. rep. NBER Working Paper No. 26882. National Bureau of Economic Research, 2020. URL: <https://www.nber.org/papers/w26882>.
- [7] Jeffrey Ely, Andrea Galeotti, and Jakub Steiner. “Rotation as Contagion Mitigation”. In: *CEPR Discussion Paper No. DP14953* (2020). URL: <https://ideas.repec.org/p/cpr/ceprdp/14953.html>.
- [8] Neil M Ferguson, Daniel Laydon, and Gemma Nedjati-Gilani et al. “Impact of non-pharmaceutical interventions to reduce COVID-19 mortality and healthcare demand”. In: *Imperial College London* (2020). URL: <https://www.imperial.ac.uk/mrc-global-infectious-disease-analysis/cov>
- [9] Will Feuer. *CNBC News article*. (accessed September 3, 2020). 2020. URL: <https://www.cnbc.com/2020/06/>
- [10] Youyang Gu. *COVID-19 Projections Using Machine Learning*. (accessed August 18, 2020). 2020. URL: <https://covid19-projections.com>
- [11] Ramon van Handel. “Probability and Random Processes”. In: *ORF 309/MAT 380 Lecture Notes* (Feb. 2016). URL: <https://web.math.princeton.edu/~rvan/ORF309.pdf>.

- [12] Omer Karin et al. “Adaptive cyclic exit strategies from lockdown to suppress COVID-19 and allow economic activity”. In: *medRxiv* (2020). DOI: [10.1101/2020.04.04.20053579](https://doi.org/10.1101/2020.04.04.20053579). eprint: <https://www.medrxiv.org/content/early/2020/04/28/2020.04.04.20053579.full.pdf>. URL: <https://www.medrxiv.org/content/early/2020/04/28/2020.04.04.20053579>.
- [13] Matt J. Keeling and Ken T. D. Eames. “Networks and Epidemic Models”. In: *Journal of The Royal Society Interface* 2.4 (2005), pp. 295–307.
- [14] S. A. Lauer et al. “The Incubation Period of Coronavirus Disease 2019 (COVID-19) From Publicly Reported Confirmed Cases: Estimation and Application”. In: *Annals of internal medicine* 172(9) (2020), pp. 577–582.
- [15] Jol Mossong et al. “Social Contacts and Mixing Patterns Relevant to the Spread of Infectious Diseases”. In: *PLOS Medicine* 5.3 (Mar. 2008), pp. 1–1.
- [16] S. Muthukrishnan and Gopal Pandurangan. “Thresholding random geometric graph properties motivated by ad hoc sensor networks”. In: *Journal of Computer and System Sciences* 76.7 (2010), pp. 686–696.

## A Appendix

### A.1 Formula for Economic Ratio

As defined in Section 2, the *economic ratio* is the *ratio* of the number of working hours of an individual under our mechanism to the number of working hours under the standard five-day working week (i.e., the (1, 5, 2) schedule), assuming that an individual works for a fixed number of hours (say, 8) on each day they are working.

**Theorem 2.** *The economic ratio for the  $(g, d, t)$  mechanism is  $\frac{7}{5} \left( \frac{d}{gd+t} \right)$ .*

*Proof.* Consider a group schedule  $(g, d, t)$ . We note that a member of group  $i$  will wait  $(g-1)d + t$  days quarantined after their final day unquarantined in a given cycle

$$\underbrace{0, 0, \dots, 0}_{d \text{ days}} \underbrace{1, 1, \dots, 1 \dots g-1, g-1 \dots g-1}_{(g-1)d \text{ days}} \underbrace{\emptyset \emptyset \dots \emptyset}_{t \text{ days}}$$

In such a cycle, there are  $gd + t$  days and each group works  $d$  days. Assuming that each day one works for a fixed number of hours, the fraction of the work hours to the total number of work hours possible is  $\frac{d}{gd+t}$ . For a standard (1, 5, 2) schedule (5-day work week), the above ratio is  $5/7$ . Hence the economic ratio for a  $(g, d, t)$  schedule is  $\frac{7}{5} \left( \frac{d}{gd+t} \right)$ .  $\square$

### A.2 Relating Reproductive Rate to Transmission Probability

Let  $C$  be the (average) number of contacts per person (we assume this value to be 13.4 throughout this paper based on [15] data) and  $D$  be the number of days a person remains infectious (we assume in this paper that this number is 11 days for COVID-19 [8]).

**Contact graph model** For the contact-graph model, one can approximately relate  $T_p$  and  $R(t)$  as follows:

$$R(t) = (1 - (1 - T_p)^D) \times C$$

This is because, each individual  $u$  can infect a given neighbor  $v$  with probability  $T_p$  every day and hence not infect with probability  $1 - T_p$ ; hence the probability that  $v$  is not infected at all for all the  $D$  days is  $(1 - T_p)^D$ . Thus the probability that  $v$  is infected during the course of  $u$ 's infection is  $1 - (1 - T_p)^D$ . Thus on average, an individual  $u$  infects  $(1 - (1 - T_p)^D)C$  individuals.

**Random Mixing Model** For the contact-graph model, one can approximately relate  $T_p$  and  $R(t)$  as follows:

$$R(t) = T_p \times C \times D$$

This is because in the random mixing model, we assume that an individual has  $C$  new contacts per day on average for each of the  $D$  days. Since each contact has a probability  $T_p$  of being infected, we have the formula. (Strictly speaking some contacts can be repeated, but since the population is large and  $D$  is small, one can assume random sampling among the population has few repeats).

### A.3 Omitted Proofs of Section 4

#### Proof of Lemma 1

*Proof.* If an infected individual  $v$  is symptomatic, then

$$D^g = \max\{0, \min\{(d-2), 5\}\} + \max\{0, \sum_{i=1,2,\dots} \min\{5 - (d + (g-1)d + t)i, d\}\}.$$

The first term  $\min\{(d-2), 5\}$  comes from the fact that the group (which goes out first) is not infectious for the first two days and that  $d-2$  cannot be more than 5 since a symptomatic patient can be put in quarantine on the 5th day (see Section 3). Also it cannot be negative, so we take the maximum between 0 and  $\min\{(d-2), 5\}$ . The second term shows the repeated process of all the groups going out for work. The term  $5 - (d + (g-1)d + t) = 5 - (gd + t)$  comes from the schedule equation (Theorem 2) and the fact that a symptomatic patient can be put in quarantine on the 5th day. Also it cannot be negative and hence the maximum function.

Also it is easy to see that  $C^g = C/g = 13.4/g$ , since we assume  $C = 13.4$ . Thus we get from Equation 1:

$$\begin{aligned} \mu_s &= T_p \cdot D^g \cdot C^g \\ &= T_p \cdot \left( d' + \sum_i d'_i \right) \cdot \frac{13.4}{g} \\ &= \frac{(13.4)T_p}{g} \cdot \left( d' + \sum_i d'_i \right) \end{aligned}$$

□

#### Proof of Lemma 2

*Proof.* If  $v$  is asymptomatic, then  $D^g$  can be calculated as follows:

$$D^g = \max\{0, \min\{d-2, 11\}\} + \max\{0, \sum_{i=1,2,\dots} \min\{11 - (d + (g-1)d + t)i, d\}\}.$$

The first term  $\min\{d-2, 11\}$  comes from the fact that the group (which goes out first) is not infectious for the first two days and that  $d-2$  cannot be more than 11 as we assume that a person can not be infectious for more than 11 days (see Section 3). The second term shows the repeated process of all the groups going out for work. The term  $11 - (d + (g-1)d + t) = 11 - (gd + t)$  comes from the equation (Theorem 2) and the fact that a person can not be infectious for more than 11 days. Both the terms cannot be negative; so the maximum function is applied before them.

$C^g$  is fixed, i.e.,  $C^g = C/g = 13.4/g$ . Thus we get from Equation 1:

$$\begin{aligned} \mu_a &= T_p \cdot D^g \cdot C^g \\ &= T_p \cdot \left( d'' + \sum_i d''_i \right) \cdot \frac{13.4}{g} \\ &= \frac{(13.4)T_p}{g} \cdot \left( d'' + \sum_i d''_i \right) \end{aligned}$$

□